

## Mirror decay of $^{75}\text{Sr}$

J. Huikari<sup>1,a</sup>, M. Oinonen<sup>2,3</sup>, A. Algora<sup>4</sup>, J. Cederkäll<sup>3</sup>, S. Courtin<sup>5</sup>, P. Dessagne<sup>5</sup>, L. Fraile<sup>3</sup>, S. Franchoo<sup>3</sup>, H. Fynbo<sup>3</sup>, W.X. Huang<sup>1</sup>, A. Jokinen<sup>1,2,3</sup>, A. Knipper<sup>5</sup>, F. Marechal<sup>5</sup>, C. Miché<sup>5</sup>, E. Nacher<sup>4</sup>, K. Peräjärvi<sup>3</sup>, E. Poirier<sup>5</sup>, L. Weissman<sup>3</sup>, J. Äystö<sup>1,2,3</sup>, and the ISOLDE Collaboration

<sup>1</sup> Department of Physics, University of Jyväskylä, P.O. Box 35, FIN-40351, Jyväskylä, Finland

<sup>2</sup> Helsinki Institute of Physics, FIN-00014 University of Helsinki, Finland

<sup>3</sup> CERN, CH-1211 Geneva 23, Switzerland

<sup>4</sup> Instituto de Física Corpuscular, CSIC - University of Valencia, E-46071 Valencia, Spain

<sup>5</sup> Institut de Recherches Subatomiques, F-67037 Strasbourg Cedex 2, France

Received: 26 September 2002 / Revised version: 24 October 2002 /

Published online: 18 February 2003 – © Società Italiana di Fisica / Springer-Verlag 2003

Communicated by D. Schwalm

**Abstract.** The  $\beta$ -decay of  $^{75}\text{Sr}$  to its mirror nucleus  $^{75}\text{Rb}$  was studied at the ISOLDE PSB facility at CERN by means of  $\beta$ -delayed  $\gamma$  and proton spectroscopy. The decay  $Q$ -value and  $\beta$ -delayed  $\gamma$  intensity were measured for the first time. These results,  $10.60 \pm 0.22$  MeV and  $4.5_{-0.7}^{+1.9}\%$ , together with accurate measurements of the  $\beta$ -decay half-life and  $\beta$ -delayed proton branching ratio yielded the Gamow-Teller strength  $0.35 \pm 0.05$  for the mirror transition. Implications of the results on studies of deformation effects and on the path of the rapid proton capture process are discussed.

**PACS.** 23.40.Hc Relation with nuclear matrix elements and nuclear structure – 21.10.Tg Lifetimes – 23.50.+z Decay by proton emission – 27.50.+e  $59 \leq A \leq 89$

### 1 Introduction

Mirror decays with  $T = 1/2$  provide an ideal laboratory for studying fine details of nuclear properties. These decays are characterized by fast Fermi and Gamow-Teller decays and short half-lives caused by high decay energies determined by Coulomb energy differences. As these transitions are strong, they can be easily identified and thus the comparison of experimental and theoretical Gamow-Teller strengths of individual transitions becomes possible [1]. So far, mirror decays have been studied with high precision only up to  $^{59}\text{Zn}$ . (See [2] and references therein.)

In the  $A = 70$ – $80$  region the breaking of isospin symmetry starts to play a significant role. It has been suggested that it may even alter the ordering of the low-lying states [3]. Furthermore, the deformation effects may drastically affect the Gamow-Teller strength distribution [4, 5].

The ground-state spin and parity of  $^{75}\text{Sr}$  are not experimentally known and the  $J^\pi$  of the  $^{75}\text{Rb}$  ground state is not firmly fixed. The ground-state  $J^\pi$  of  $^{75}\text{Rb}$  has been determined as  $(3/2^-)$  or  $(5/2^-)$  by Kern *et al.* via a  $\beta$ -decay study [6]. The in-beam experiment by Gross *et al.* suggests  $(3/2^-)$  for the  $^{75}\text{Rb}$  ground state [7]. So far, the  $\beta$ -decay half-life [8, 9] and  $\beta$ -delayed proton decay [8] for

$^{75}\text{Sr}$  have been measured only with modest accuracies. In this paper we report on the first detailed study of the mirror  $\beta$ -decay of  $^{75}\text{Sr}$ , extending the systematical study of mirror decays up to the region of large deformations.

### 2 Experimental information

$^{75}\text{Sr}$  isotopes were produced via spallation reactions in a Nb-foil target by using pulsed 1 GeV and 1.4 GeV proton beams from the PS Booster at CERN and mass separated at the ISOLDE facility [10]. SrF molecules were created by adding  $\text{CF}_4$  gas into the target, and ionized in a surface ionisation ion source in order to obtain an isotopically clean  $\text{SrF}^+$  beam. The average yield measured for  $^{75}\text{SrF}^+$  was 5.4 ions/s ( $= 2.5$  ions/ $\mu\text{C}$ ) over a total measurement time of 21 h.

The  $\text{SrF}^+$  beam was implanted on a movable aluminized Mylar tape in order to remove long-living daughter activities from the source position. The tape was moved after every 20th proton pulse. The detection set-up used for the half-life and  $\beta$ -delayed  $\gamma$ -rays consisted of a cylindrical plastic scintillator for  $\beta$  particles and three HPGe detectors for  $\gamma$ -rays. Another set-up for  $\beta$ -delayed protons and  $\gamma$ -rays consisted of the FUTIS array [11] with 15 Si ( $300 \mu\text{m}$ ) detectors, with a transmission-type

<sup>a</sup> e-mail: jussi.huikari@phys.jyu.fi

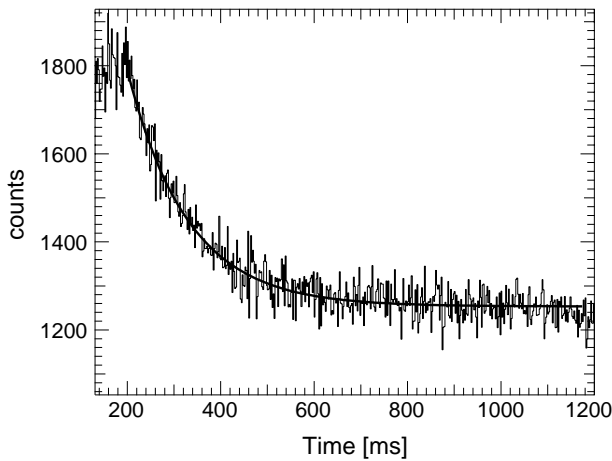


**Fig. 1.** The scintillator time spectrum used to determine the half-life of  $^{75}\text{Sr}$ .

Si ( $500\ \mu\text{m}$ ) detector behind the implantation position and a 20 mm thick planar Ge detector. The combination of the transmission detector and the planar detector also formed a  $\beta$  telescope for a  $Q_{\text{EC}}$  measurement. Both energy and time signals were recorded in a list-mode from each detector. The time behaviour of the signals relative to the proton pulse impact in the target was also recorded (the so-called timestamp spectrum) in order to determine the half-life values.

The efficiency calibrations for all the  $\gamma$  detectors were made by using an absolutely calibrated  $^{133}\text{Ba}$  source. In the FUTIS set-up two energy amplifications were used for the planar Ge detector, one for  $\gamma$ -rays and the other with lower amplification for recording the positron energy spectrum. An on-line source of  $^{20}\text{Na}$  was used to obtain energy and absolute efficiency calibration for the FUTIS array. Particularly, the  $\beta$ -delayed 1633 keV  $\gamma$  transition in  $^{20}\text{Na}$  decay detected in the planar Ge detector was used to obtain the efficiency calibration for the FUTIS array. The counting rate was kept small by selecting a time window from the end of the cycle (900–1000 ms) to avoid dead-time effects in the planar Ge detector.

### 3 Experimental results

#### 3.1 $\beta$ -decay half-life

Since our experiment was carried out with two different set-ups, two independent half-life measurements were performed. The half-life of  $^{75}\text{Sr}$  was determined from the time behaviour of the  $\beta$ -transmission spectra measured with the scintillator of the  $\beta$ - $\gamma$  set-up (fig. 1) as well as with the Si-detector of the FUTIS set-up. In order to extract the  $\beta$ -decay half-life from the data, only the decay part was used as the growth-in part included the delay caused mainly by the diffusion and effusion of Sr out of the ISOLDE target. The half-life was extracted using the procedure described in [12]. The daughter of  $^{75}\text{Sr}$ ,  $^{75}\text{Rb}$ , has a half-life of 19 s and was included in the fit.

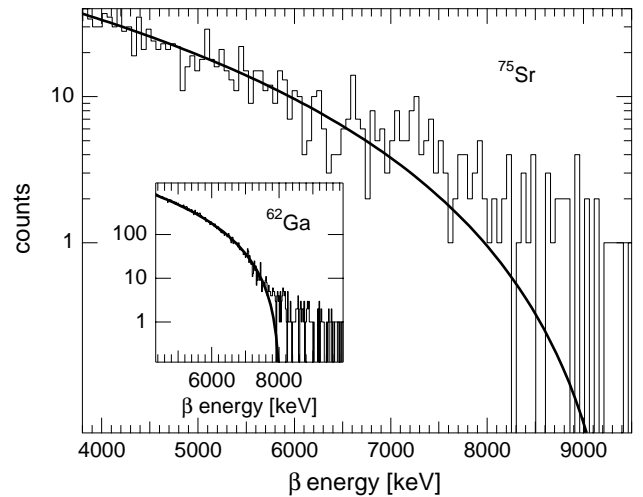


**Fig. 2.** The positron energy spectrum of the  $^{75}\text{Sr}$  decay. The insert graph shows the  $^{62}\text{Ga}$  positron energy spectrum used for the energy calibration.

The granddaughter,  $^{75}\text{Kr}$ , has a long half-life (4.5 min) and its effect, therefore, was considered negligible. The half-lives determined from these two experiments were  $87 \pm 3$  and  $89 \pm 5$  ms. Their weighted average,  $88 \pm 3$  ms, was adopted as a  $\beta$ -decay half-life of  $^{75}\text{Sr}$ .

#### 3.2 Total decay energy

The total decay energy was measured by using a low amplification signal from the planar Ge detector of the FUTIS set-up. The background  $\gamma$ -rays were removed by gating the planar Ge with the transmission Si detector. The contamination from long-living daughters was reduced by gating the Si and Ge detectors with the timestamp spectrum.

In order to extract the endpoint of the  $\beta$  spectrum, the fitting procedure described in [13,14] was used. The following equation was used in the fit:

$$N_0 S(x) = N_0 (a + bx + x^2)(x - x_0), \quad (1)$$

where  $N_0$  is the normalization factor,  $x$  is the channel number, and  $a$ ,  $b$  and  $x_0$  are shape parameters. In this procedure, the high-energy part of the known  $\beta$  spectrum is fitted with all parameters free. The fitting range was chosen above the daughter and contaminant endpoint energies. Once the shape parameters are found, they are fixed for all subsequent analyses. After this, all the other spectra, calibration and unknown ones, are fitted with the 2-parameter function  $N_0 S(cx)$ , where  $N_0$  is the normalization and  $c$  is the stretch factor taking into account the differing total decay energies.

In the present experiment, the decay of  $^{62}\text{Ga}$  provided the known spectrum (fig. 2). The use of the on-line produced  $^{62}\text{Ga}$  as a reference minimized systematic errors, taking into account the  $\beta$  energy loss in the material between the planar Ge and the source as well as in the dead

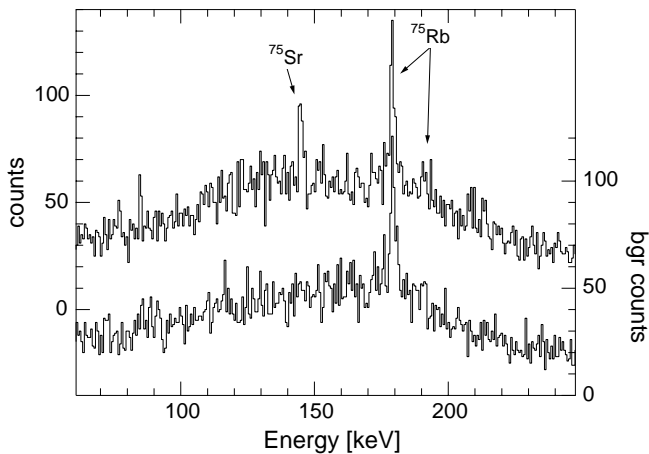


**Fig. 3.** The  $\gamma$  spectrum of  $A = 75$  decays. The upper part is  $^{75}\text{Sr}$  + background and the lower part is the long-lived background.

layer of the planar Ge. In addition, this included the summing due to 511 keV  $\gamma$ -rays in the calibration. The effect of the  $\beta$  feeding to the excited states in  $^{75}\text{Rb}$  was estimated to be negligible.

Neutron-induced  $\gamma$ -rays of  $^{56}\text{Fe}$  originating from the FUTIS vacuum chamber were exploited in the energy calibration. This provided the slope of the calibration which was further normalized to the endpoint energy of  $^{62}\text{Ga}$ . The calibration was checked with on-line sources of  $^{50}\text{Mn}$  and  $^{20}\text{Na}$  (see also [14]). The measured  $Q_{\text{EC}}$ -value for  $^{75}\text{Sr}$  was  $10.60 \pm 0.22$  MeV.

### 3.3 $\beta$ -delayed $\gamma$ -decay

In the present study,  $\gamma$ -rays were measured in coincidence with  $\beta$ 's. Additional cleaning of background was performed by gating the  $\gamma$  spectrum with the time window set to 45–600 ms ( $^{75}\text{Sr}$  + background) and 645–1200 ms (background). This allowed the identification of long-living daughter  $\gamma$ -rays in the spectrum (fig. 3).

Only one short-living transition, 144 keV, was observed in the  $\gamma$ -ray spectrum. The time behaviour of the 144 keV peak was similar to the one observed for positrons. No other short-living  $\gamma$  peaks with a  $3\sigma$  confidence limit were identified in the spectrum. The  $\beta$  feeding to the 144 keV level could be extracted from both experiments with the  $\beta$ - $\gamma$  and the FUTIS set-ups. The values obtained were  $4.6 \pm 0.9\%$  and  $4.4 \pm 1.3\%$ , respectively.

No evidence of  $\beta$  feeding to higher-lying levels of  $^{75}\text{Rb}$  was observed in the present experiment. However, due to a limited  $\gamma$ -ray detection efficiency for higher energies, a small feeding by  $\beta$ -decay to higher-energy levels cannot be ruled out. An internal conversion may also have had an effect on measured  $\beta$  feeding to the 144 keV level. The multipolarity of the 144 keV transition is most likely a mixed  $M1/E2$ . Although the faster  $M1$  should dominate, the maximum internal conversion coefficient can be estimated if assuming a pure  $E2$  transition. In this case, the total conversion coefficient would be 0.22. Due to this fact,

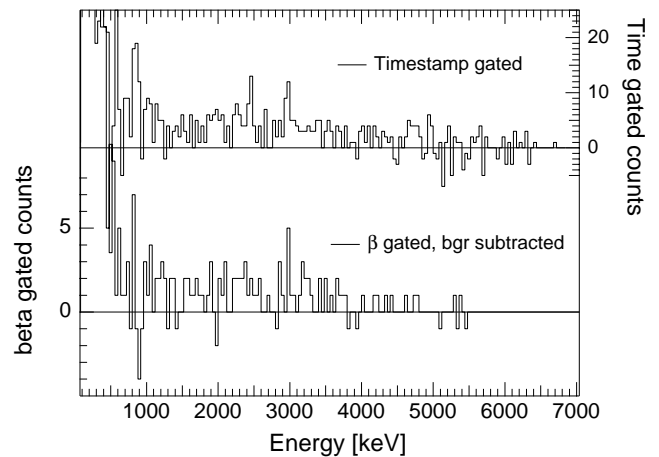


**Fig. 4.** The proton energy spectra of the  $^{75}\text{Sr}$  decay. The upper part shows the timestamp-gated single spectrum and the lower part shows  $\beta$ - and the timestamp-gated proton spectrum. See the text for details.

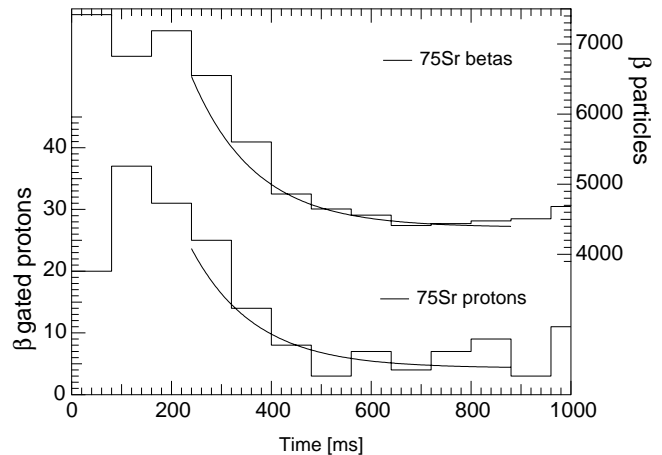


**Fig. 5.** The positron and proton timestamp spectra of  $^{75}\text{Sr}$  decay. The solid line is a fit to extract the total number of decays in both cases.

the  $\beta$  feeding to the 144 keV level can be higher than measured here. This possibility was taken into account when calculating the uncertainty of the branching ratio. Thus, the weighted average of  $4.5^{+1.9}_{-0.7}\%$  was adopted as a final branching ratio.

### 3.4 $\beta$ -delayed proton decay

The FUTIS array was used to measure  $\beta$ -delayed protons in singles mode and in coincidence with positrons. The Si detector opposing the FUTIS array provided the  $\beta$  signal. The spectrum measured with the FUTIS array is shown in fig. 4. The upper part of the figure displays counts above 1 MeV with a short half-life. In this spectrum, the long-living background (time window 725–1000 ms) was subtracted from the short-living part (time window 75–350 ms). The lower part of fig. 4 shows a spectrum gated with positrons with the same time windows as above. Since the counts in the upper spectrum show the

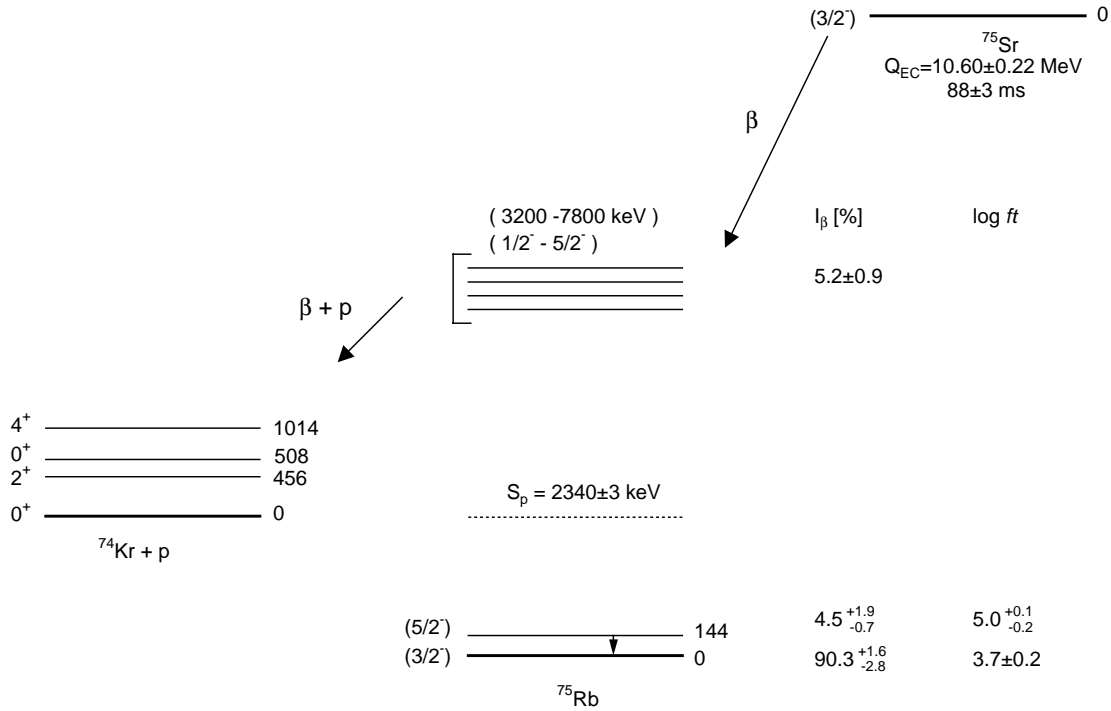


Fig. 6. Decay scheme of  $^{75}\text{Sr}$ .

Table 1. The  $\beta$ -decay of  $^{75}\text{Sr}$ . See the text for details.

Level (keV)	$J^\pi$	$I_\beta$ (%)	$\log ft$	$ \langle\sigma\tau\rangle $
0	$(3/2^-)$	$90.3^{+1.6}_{-2.8}$	$3.7 \pm 0.2$	$0.35 \pm 0.05$
144	$(5/2^-)$	$4.5^{+1.9}_{-0.7}$	$5.0^{+0.1}_{-0.2}$	$0.20^{+0.04}_{-0.02}$
$p$ unbound		$5.2 \pm 0.9$		

same time behaviour as the positrons, they were assigned to the  $\beta$ -delayed proton decay of  $^{75}\text{Sr}$ .

For the determination of the  $\beta$ -delayed proton intensity, the energy window of 850–5500 keV was used on the FUTIS array. The  $\beta$ -delayed proton branch was extracted by generating the time-gated spectra for positrons as well as for protons by gating the FUTIS array with the  $\beta$  transmission peak of the Si detector and by using the energy window mentioned above. In order to include protons following the electron capture decay, the proton timestamp spectrum was generated also using the energy window of 1500–5500 keV on the FUTIS array. The lower limit chosen was 1500 keV due to a possible presence of positrons at lower energies. The total number of protons obtained from this spectrum was compared with the  $\beta$ -gated proton timestamp spectrum (energy window 1500–5500 keV). This ratio was used to correct the  $\beta$ -delayed proton intensity. Both timestamp spectra are shown in fig. 5. The total number of positrons and protons were extracted from these timestamp spectra by fitting them with the same exponential function as obtained for

the half-life and  $\beta$ -delayed  $\gamma$ -ray measurements. Here the half-life was fixed as 88 ms. Thus, the only free parameters were the number of particles and the background. Hence, the final  $\beta + \text{EC}$  delayed proton decay branching ratio obtained was  $5.2 \pm 0.9\%$ .

## 4 Discussion

Table 1 presents the measured  $\beta$ -decay properties of  $^{75}\text{Sr}$ . The decay scheme shown in fig. 6 summarizes the  $\beta$ -decay properties of  $^{75}\text{Sr}$  as measured in the present experiment.

Our result for the  $\beta$ -decay half-life of  $^{75}\text{Sr}$ ,  $88 \pm 3$  ms, is in agreement with the previous values,  $71^{+71}_{-24}$  ms [8] and  $80^{+400}_{-40}$  ms [9], and the uncertainty is smaller by an order of magnitude. The measured  $Q_{\text{EC}}$ -value,  $10.60 \pm 0.22$  MeV, agrees with the value obtained from the FRDM calculation, 10.7 MeV [15], and from the mass systematics from ref. [16],  $10.6 \pm 0.3$  MeV.

The present experiment measured the  $\beta$ -delayed  $\gamma$ -ray de-exciting the  $^{75}\text{Rb}$  level for the first time. As the time behaviour of the measured 144 keV transition follows that of the positrons of  $^{75}\text{Sr}$  decay, it was assigned to be due to a  $(5/2^-)$  level of  $^{75}\text{Rb}$  de-exciting to the ground state. The  $\log ft$  values deduced for the 144 keV level and the ground state are 5.0 and 3.7, respectively. The stronger transition to the ground state suggests superallowed character. Therefore,  $J^\pi$  of the ground state of  $^{75}\text{Sr}$  has to be the same as that of the  $^{75}\text{Rb}$  ground state. If we adopt spins and parities from [7], the  $^{75}\text{Sr}$  ground state must have  $J^\pi = (3/2^-)$ . Both the earlier  $\beta$ -decay work by Kern [6]

and the theoretical work by Hamamoto [17] support this assignment.

The measurements of the half-life,  $Q_{\text{EC}}$ -value, and branching ratios allowed us to determine the Gamow-Teller matrix elements,  $|\langle\sigma\tau\rangle|$ , for the transitions. The formula below was used in the calculation:

$$(1 + \delta_R)ft = \frac{C}{(1)^2(1 - \delta_C) + R^2\langle\sigma\tau\rangle^2}, \quad (2)$$

where the following values for the radiative correction ( $1 + \delta_R$ ), the correction for isospin impurity ( $1 - \delta_C$ ), the constant  $C$  and the axial-vector to vector coupling constant ratio  $R = g_A/g_V$  were used:

$$(1 + \delta_R) = 1.026 \text{ [18]},$$

$$(1 - \delta_C) = 0.997(3) \text{ [19]},$$

$$C = 6145(4) \text{ [20]},$$

$$|g_A/g_V| = 1.266(4) \text{ [21]}.$$

The ground-state and excited-state Gamow-Teller matrix elements were determined to be  $0.35 \pm 0.05$  and  $0.20_{-0.02}^{+0.04}$ , respectively. The values obtained from this experiment are presently the most accurate ones for mirror nuclei in the mass region  $A > 61$ . The experimental GT-matrix element of the mirror transition follows the systematical trend of the measured values of lower-mass nuclei [2].

In the framework of the HF + BCS + QRPA formalism, the low-energy part of the GT strength distribution in odd- $A$   $N \sim Z$  nuclei is due to 1-quasiparticle excitations involving the single odd neutron [22]. The higher-energy part is mainly due to more collective excitations and can possibly be used to distinguish between oblate and prolate deformations of a nucleus; one of the best candidates being the  $N = Z$  nucleus  $^{76}\text{Sr}$  [5]. The structure of the collective (3 quasiparticle) GT strength distribution of a corresponding  $N = Z + 1$  nucleus is similar but shifted towards higher excitation energies [22]. In the case of  $^{75}\text{Sr}$ , the high-energy part of the GT strength would be at  $> 4$  MeV excitation energies [23] corresponding to  $E_p > 1.5$  MeV if proton emission directly populates the ground state of  $^{74}\text{Kr}$ . Therefore, the experimentally observed  $\beta$ -delayed proton spectrum seems to probe the part of the GT strength distribution that directly populates 3-quasiparticle induced states in  $^{75}\text{Rb}$ . This indicates  $^{75}\text{Sr}$  to be a highly promising case for studying the deformation effects as the large proton branching ratio should compensate the lower production cross-section compared to  $^{76}\text{Sr}$ .

The measured half-life of  $^{75}\text{Sr}$  is a factor of 2 shorter than the QRPA value used for the rp-process calculations [15]. However, it does not play a significant role as the speed of the rp-process flow is mainly determined by the  $\beta$ -decay half-life of neighbouring  $^{76}\text{Sr}$  considered to be a possible waiting-point nucleus ( $T_{1/2} = 9$  s) [15]. A way to bypass the waiting point would be a 2-proton capture on  $^{75}\text{Sr}$  bringing the masses of  $^{75}\text{Sr}$ ,  $^{76}\text{Y}$  and  $^{77}\text{Zr}$

into play. Recently,  $^{76}\text{Y}$  was observed at GSI [9]. No evidence of proton-bound nature of  $^{77}\text{Zr}$  has been obtained so far. However, there is strong theoretical support for a proton-bound  $^{77}\text{Zr}$  ground state as the most mass models predict the proton dripline in the  $^{72-75}\text{Zr}$  region [24]. Hence, our first-ever measurement of the mass of  $^{75}\text{Sr}$  via its  $Q_{\text{EC}}$ -value determination forms a basis for further research on a possible by-pass mechanism of the waiting point of  $^{76}\text{Sr}$ .

To conclude, we have measured the  $\beta$ -decay half-life of  $^{75}\text{Sr}$  at the ISOLDE mass separator facility via two independent ways, accurate to 3.4%. For the first time, we have measured the total  $\beta$ -decay energy and observed  $\beta$ -delayed  $\gamma$ -decay. These values, together with the measured  $\beta$ -delayed proton decay branching ratio, have been used to extend the systematics of the GT matrix elements of mirror decays towards the region of high deformation. The large  $\beta$ -delayed proton branch indicates strong feeding to the high-lying states of  $^{75}\text{Rb}$ , giving a qualitative insight into nuclear deformation effects.

A. Jokinen acknowledges the support of the Academy of Finland. Partial support from the EC HPMFCT-1999-00394 contract is acknowledged by A. Algora. The support from Access to Research Infrastructures Improving Human Potential Programme (HPRI-CT-1998-00018) is acknowledged by J. Huikari.

## References

1. G. Martinez-Pinedo *et al.*, Phys. Rev. C **53**, R2602 (1996).
2. M. Oinonen *et al.*, Phys. Rev. C **56**, 745 (1997).
3. P. Urkedal, I. Hamamoto, Phys. Rev. C **58**, R1889 (1998).
4. F. Frisk *et al.*, Phys. Rev. C **52**, 2468 (1995).
5. P. Sarriguren, Nucl. Phys. A **691**, 631 (2001).
6. B. Kern, Phys. Rev. C **28**, 2168 (1983).
7. C.J. Gross *et al.*, Phys. Rev. C **56**, R591 (1997).
8. B. Blank *et al.*, Phys. Lett. B **365**, 8 (1995).
9. P. Kienle *et al.*, Prog. Part. Nucl. Phys., **46**, 73 (2001).
10. E. Kugler *et al.*, Nucl. Instrum. Methods Phys. Res. A **70**, 41 (1992).
11. M. Oinonen *et al.*, JYFL Annual report (1996) p. 16; H. Fynbo *et al.*, Nucl. Phys. A **677**, 38 (2000).
12. M. Oinonen *et al.*, Phys. Rev. C **61**, 35801 (2000).
13. C.N. Davids *et al.*, Phys. Rev. C **19**, 1463 (1979).
14. L. Weissman *et al.*, Phys. Rev. C **65**, 44321 (2002).
15. H. Schatz *et al.*, Phys. Rep. **294**, 167 (1998).
16. G. Audi, A. Wapstra, Nucl. Phys. A **595**, 409 (1995).
17. I. Hamamoto, Phys. Rev. C **60**, 11305 (1999).
18. G.T. Ewan *et al.*, Nucl. Phys. A **352**, 13 (1981).
19. D.H. Wilkinson *et al.*, Phys. Rev. C **18**, 401 (1978).
20. I. Towner *et al.*, *ENAM 95 Proceedings, Arles, France*, edited by M. de Saint Simon, O. Sorlin (Editions Frontières, Gif-sur-Yvette, 1995) p. 711.
21. K. Schreckenbach *et al.*, Phys. Lett. B **349**, 427 (1995).
22. P. Sarriguren *et al.*, Phys. Rev. C **64**, 064306 (2001).
23. P. Sarriguren *et al.*, private communication (2002).
24. G. Lalazissis, Nucl. Phys. A **679**, 481 (2001).